Theoretical studies on carbonyl halide-water complexes

Nobuaki Tanaka [a,*], Takumi Tamezane [a], Hiromasa Nishikiori [a], Tsuneo Fujii [a], Wade N. Sisk [b]

[a] *Department of Environmental Science and Technology, Faculty of Engineering, Shinshu University, 4-17-1 Wakasato, Nagano, Nagano 380-8553, Japan*

[b] *Chemistry Department, University of North Carolina at Charlotte*

9201 University City Blvd., Charlotte, NC 28223-0001, USA

Received

Abstract

Theoretical investigations of carbonyl halide complexes, FXCO-H_2O (X = F, Cl) have been performed. Structures and vibrational frequencies are determined at the MP2 and B3LYP levels of theory with basis sets up to aug-cc-pVTZ. Two conformers of FXCO-H_2O complex have been found. The structures of FXCO-H_2O complexes are calculated to be (I) coplanar hydrogen-bonded and (II) angular with C···O and O···H contacts. Complexation causes the C=O bond elongation and the C-F bond contraction. NBO analysis revealed intermolecular charge transfers occur followed by intramolecular charge rearrangement.

Key words: Ab initio, carbonyl halide, NBO, complex, water

[*] Corresponding author. Fax: +81-26-269-5550.

E-mail address: ntanaka@gipwc.shinshu-u.ac.jp (N. Tanaka).

1. Introduction

To protect the stratosphere from the ozone depletion catalyzed by a chlorine atom, chlorofluorocarbons CFCs have been replaced by substituents, hydrofluorocarbons HFCs [1]. Recently, hydrofluoroethers HFEs are also under consideration for use. These measures have resulted in deceleration of ozone layer destruction due to the chlorine atom released from the photolysis of CFCs. However, HFCs have potential as a green house molecule [2,3]. Of the oxidation products CFCs, HFCs and HFEs, calbonyl difluoride or carbonyl chloride fluoride is observed as a common product [4-8]. Therefore, the properties and the role of carbonyl halides in atmosphere should be known. The stratospheric abundance has been measured for F_2CO, a fluorine atom reservoir [9]. The threshold energies of the first electronic transition A←X of carbonyl halides were observed to be 4.86, 4.79 and 4.1 eV for F_2CO [10], FClCO [11] and Cl_2CO [12], respectively. In the stratosphere, photodissociation will be the key decomposition process of the molecules. Photolysis quantum yields at 193 nm were measured to be 0.94, 0.98 and 1.0 for F_2CO, FClCO and Cl_2CO, respectively [13-15]. Maul et al. reported the three body decay dynamics of FClCO [16] and Cl_2CO [17]. As the photon energy increases, the three-body decay becomes dominant over the two-body decay. In the lower humid atmosphere, the interaction with water should be important. A theoretical study on the F_2CO reaction with water reveals the primary concerted reaction to form fluoroformic acid and HF [18]. A recent study on the phosgene-water complex shows the complex has two minima on the potential energy surface at the MP2/aug-cc-pVTZ level of theory [19]. The most stable conformer is found to be the T-shape complex where the water oxygen interacts with the phosgene C=O bond.

Weakly bound hydrogen bonded complexes have attracted many researchers [20-23]. Water is a good probe to explore the potential surface and it is widely known that complexation with the water molecule causes the changes in the vibrational frequency and the IR intensity. Complexes possessing large interaction energy may enhance the green house effect [24]. More weakly bound van der Waals complexes of F_2CO with Ar [25,26], N_2 [26], Cl_2 [27] and IF [28] have been investigated by infrared matrix isolation and ab initio studies. Conformations of the F_2CO complexes are classified into the T-shape and the coplanar structures. The F_2CO-Ar and F_2CO-N_2 complexes have T-shape structures while the F_2CO-Cl_2 and F_2CO-IF complexes have planar structures. In F_2CO-N_2, the N_2 molecular axis is perpendicular to the F_2CO molecular plane.

In this paper, we discuss the structure and energetics of the carbonyl halide-water complexes, FXCO-H_2O (X = F, Cl), obtained by the MP2 and B3LYP calculations. Comparison with the corresponding Cl_2CO-H_2O complex will be made.

2. Method of calculation

Geometry optimizations are performed at the second-order Møller-Plesset theory, MP2 using PC GAMESS version [29] of the GAMESS (US) QC package [30] and GAUSSIAN 03W [31]. For weak bonding, both diffuse and polarization functions must be included in the basis set, so we used the 6-311++G(2d,2p) and Dunning's correlation consistent triple zeta basis set augmented with diffuse functions, aug-cc-pVTZ) [32,33] obtained from the Extensible Computational Chemistry Environment Basis Set Database, Version 7/30/02 [34]. After structural optimization, single-points calculations are

performed with the coupled-cluster theory, CCSD(T)/6-311++G(2d,2p) level and the MP2 level using the basis sets up to aug-cc-pV5Z. Analysis of the charge distribution and charge-transfer processes was performed using the natural bond orbital (NBO) partitioning scheme [35] with the aug-cc-pVTZ basis set. For comparison the DFT calculations were employed using the GAUSSIAN 03W program. The basis set superposition error (BSSE) was calculated according to the counterpoise (CP) method proposed by Boys and Bernardi [36].

3. Results and discussion

3.1. Geometry and interaction energy of complex

Structural parameters of F_2CO and FClCO are given in Table 1. The calculated structural parameters of F_2CO and FClCO are in good agreement with experimental values [37,38]. Firstly geometry optimizations of the complex were performed at the MP2/6-311++G(d,p) level starting from different initial positions of the two monomers, which converged to two minima. Based on the structures, further optimization at higher level and DFT optimization were employed. Two stable conformations calculated with the MP2/aug-cc-pVTZ level are shown in Figure 1 and geometric parameters are listed in Tables 2 and 3 for the F_2CO-H_2O and FClCO-H_2O complexes, respectively. It is seen that the bond lengths and angles for the complexes are slightly perturbed from their values in the monomers. In complex I, FXCO and H_2O form a coplanar hydrogen bonding. For FClCO, H_2O locates on the F side of the molecule. The calculated distances for

O2···H6 and O2···O5 are 2.086 and 3.033 Å, respectively, for F_2CO-H_2O and 2.087 and 3.044 Å, respectively, for FClCO-H_2O, which are the properties for the moderate hydrogen bond [22]. The C1-O2 and O5-H6 bonds are elongated by 0.0036 and 0.0025 Å, respectively upon formation of the hydrogen bond, while the C1-F3 and C1-F4 bonds are contracted by 0.0065 and 0.0046 Å, respectively for the F_2CO-H_2O complex. The contraction is larger for the C-F bond close to the H_2O molecule. The angles are slightly sensitive to the complexation. Similar changes are predicted for the FClCO-H_2O complex. In complex II of FXCO-H_2O, the molecular plane of H_2O tilts toward the F atom in contrast to the most stable Cl_2CO-H_2O complex where H_2O molecular plane is almost perpendicular to that of Cl_2CO [19]. The distances for C1···O5, O2···O5 and O2···H6 are calculated to be 2.644, 2.950 and 2.905 Å, respectively, for the F_2CO-H_2O complex and 2.758, 2.937 and 2.752 Å, respectively, for the FClCO-H_2O complex. The contractions of the C-F and C-Cl bonds are smaller compared with those of the complex I. Both O5-H6 and O5-H7 bonds are lengthened at the MP2 level, while the O5-H6 bond is lengthened and the O5-H7 bond is contracted at the B3LYP level. Compared with the MP2 calculation, the intermolecular distances optimized at the B3LYP level are longer for both complexes. There is a small difference in the equilibrium structures of the complexes obtained by the MP2 and B3LYP calculations.

(Fig. 1 and Tables 1-3)

Calculated interaction energies including BSSE correction for the complexes are listed in Table 4. As shown complex II is more stable than complex I irrespective of the calculation levels. With the aug-cc-pVTZ basis set, DFT calculation underestimates the energies compared with the MP2 calculation presumably due to the lack of contribution of dispersion interactions [39]. The influence of higher correlation effects on the energies

was investigated by the single point calculation for the MP2 geometry. With the 6-311++G(2d,2p) basis set, the energies obtained at the MP2, MP4SDTQ and CCSD(T) levels are comparable. The CBS limit energies at the MP2 level are obtained using the equation $E(X) = E_{CBS} + A\exp(-(X-1)) + B\exp(-(X-1)^2)$ [40] with the correlation-consistent basis sets, aug-cc-pVXZ (X = T, Q and 5). Convergence is faster for the complex I. The calculation for the complex II requires large basis sets to evaluate the dispersion interaction. At the MP2 level, the interaction energies are calculated to be –4.17, –3.52 and –3.18 kcal mol^{-1} for the angular F_2CO, FClCO and Cl_2CO complexes, respectively. The HF/aug-cc-pV5Z energy for Cl_2CO-H_2O was calculated to be –1.10 kcal mol^{-1}. The complex correlation energy increases in the order F_2CO-H_2O, FClCO-H_2O and Cl_2CO-H_2O, indicative of the larger contribution of the dispersion energy for chlorine compounds. This trend is also supported by the fact that the polarizabilities of F_2CO, FClCO and Cl_2CO are calculated to be 14.0, 23.4 and 31.9 au, respectively, at the MP2/aug-cc-pVTZ level.

(Table 4)

3.2. Vibrational frequencies and intensities

To elucidate the influence of the complexation on the vibrational spectra of the monomers forming complexes, the accuracy of the calculations are compared in Table 5 for the vibrational frequencies and infrared intensities of the monomers at the MP2 and B3LYP levels of theory with the aug-cc-pVTZ basis set. The calculated values of the vibrational frequencies at the MP2 level are in better agreement with the experimental values [41,42] than those obtained at the B3LYP level. The calculated values for the O-H stretching vibrations of the water deviate significantly from experimental values. The calculated

frequencies give reasonable predictions for the complex vibrations possessing small anharmonicities. Tables 6 and 7 show unscaled vibrational frequencies and infrared intensities of the complexes I and II calculated using the aug-cc-pVTZ basis set, respectively. In our previous studies it was shown that the complexation leads to the substantial changes in the vibrational characteristics for the vibrations of the monomer bonds not only participating in the complexation but also spectators [19]. As a result of geometry change after complexation, the asymmetric and symmetric O-H stretching and C1-O2 stretching vibrational frequencies decrease, while the other vibrational frequencies increase for complex I. Among the latter vibrations the CF_2 symmetric stretching and C-F stretching vibrations are most sensitive to the complexation for the F_2CO-H_2O and FClCO-H_2O complexes, respectively.

The basic trend of the shifts is the same as that of the hydrogen-bonded H_2CO-H_2O complex [43]. For complex II, both asymmetric and symmetric O-H stretching vibrational frequencies are shifted to lower frequencies, corresponding to the O5-H6 and O5-H7 bond elongation. Out-of-plane deformation vibrations are shifted to lower frequencies. Similar to complex I, the C-F and C-Cl stretching frequencies are blue-shifted upon the complexation and the intensities of these bands decrease.

In addition to the intramolecular vibrations, there are six more intermolecular vibrations, the stretching vibration, three torsional vibrations and two in-plane bending vibrations.

(Tables 5-7)

3.3. Charge distribution

To clarify the nature of the complexation, the NBO analysis was carried out. Table 8 gives the natural atomic charges (q) for monomers and the changes in natural atomic charges (Δq) for complexes calculated with the aug-cc-pVTZ basis set. The negativity of oxygen atoms O2 and O5 increases in complexes in comparison with those of the monomer. In complex I, the positivity of the C1 and H6 atoms greatly increase. The in-contact bonds become more polarized. On the other hand, in complex II the hydrogen atoms lose charges while the fluorine atoms gain charge. The net charge transfer (CT) was evaluated to be 3.6 (3.8) me for F_2CO (FClCO) to H_2O for complex I and 3.9 (3.9) me for H_2O to F_2CO (FClCO) for complex II.

(Table 8)

Tables 9 and 10 list the second-order perturbation energies and the changes in electron density in the orbitals for complexes I and II, respectively. The second-order perturbation analysis of the Fock matrix indicated the important intermolecular interactions (1) $n_{1\ O2} \rightarrow \sigma^*_{O5\text{-}H6}$ and (2) $n_{2\ O2} \rightarrow \sigma^*_{O5\text{-}H6}$ for complex I and (1) $n_{2\ O5} \rightarrow \pi^*_{C1\text{-}O2}$ for complex II. For complex I, the primary effect is the charge transfer from carbonyl oxygen lone pair, $n_{2\ O2}$, of FXCO to the O5-H6 antibonding orbital, $\sigma^*_{O5\text{-}H6}$ of water. An increase in the electron density in $\sigma^*_{O5\text{-}H6}$ orbital leads to weakening of the O5-H6 bond accompanied by its elongation. Concomitant structural reorganization of the electron donor takes place. The $\pi^*_{C1\text{-}O2}$ orbital gains population due to the increase of the $n_{3\ F3} \rightarrow \pi^*_{C1\text{-}O2}$ and $n_{3\ X4} \rightarrow \pi^*_{C1\text{-}O2}$ interactions. The $\sigma^*_{C1\text{-}F3}$ and $\sigma^*_{C1\text{-}X4}$ orbitals lose population mainly due to the decrease of $n_{2\ O2} \rightarrow \sigma^*_{C1\text{-}F3}$ and $n_{2\ O2} \rightarrow \sigma^*_{C1\text{-}X4}$ interactions. The population increases in the $\sigma^*_{C1\text{-}O2}$, $\pi^*_{C1\text{-}O2}$, and $n_{2\ O2}$ orbitals cause the elongation of the C1-O2 bond and the red shifts of the C1-O2 stretching vibrational frequency, while the

population decreases in the $\sigma^*_{C1\text{-}F3}$, $\sigma^*_{C1\text{-}X4}$, $n_{3\ F3}$, and $n_{3\ X4}$ orbitals lead to contractions of the C1-F3 and C1-X4 bonds and the blue shifts of the C-F and C-X stretching vibrational frequencies. The CT interactions in complex II is similar to the T-shape Cl_2CO-H_2O complex. For complex II, the charge transfer from the water lone pair, $n_{2\ O5}$, to the C1-O2 antibonding orbital, $\pi^*_{C1\text{-}O2}$, of HXCO is noticeable. It leads to the C1-O2 bond weakening and elongation. Compared with the complex I, the intramolecular charge rearrangement is smaller for the complex II, which causes smaller structural changes from the monomer after the complexation.

(Tables 9 and 10)

3.4. Comparison of potential energy surfaces of carbonyl halides

Since the angular conformer is found to be the most stable complex, we concentrate on this conformation and compare the potential energy surfaces of three carbonyl halides. Fig. 2 shows the potential energy changes at the CCSD(T)/6-311++G(2d,2p) level as a function of the dihedral angle $\varphi_{C1O5H6H7}$ including the result for the Cl_2CO-H_2O complex for comparison. The H_2O complex with F_2CO has the double-well potential, while there is no stationary point for the Cl side of the FClCO-H_2O complex. This will be attributed to the difference in the C-F and C-Cl bond lengths. However, the barrier height to flipping for the former complex is very small.

(**Fig. 2**)

Fig. 3 shows the potential energy changes at the MP2/6-311++G(2d,2p) level as a function of the intermolecular distance r_{C1O5}. For the FClCO-H_2O complex, the conformation change occurred at the distance longer than 5.0 Å from perpendicular to planar with a

Cl4···O5 interaction. Probably due to the symmetry of the molecule the dipole-dipole interaction favors the planar conformation at the longer distance.

(**Fig. 3)**

Fig. 4 illustrates the comparison of the electrostatic potentials of three carbonyl halides at 0.015 a.u. where the light and dark gray surfaces represent the positive and negative potentials, respectively. Since the electrostatic potential is the energy of a positive test charge at a given location, the oxygen and hydrogen atoms of the water molecule should favor the positive and negative regions of the potential, respectively. The negative potentials spread around the O2 atom where a preferable hydrogen bond will be made. The positive potential for F_2CO deviates along the axis perpendicular to the molecular plane, while for FClCO and Cl_2CO it deviates along the C-Cl bond. It is reasonable that the C···O approaches of water along the axis perpendicular to the carbonyl halide molecular plane give the most stable T-shape complexes with C1···O5 and O2···H6 interactions. For Cl_2CO, the Cl atom possesses another possible point to form the Cl···O complex.

(**Fig. 4)**

4. Conclusions

Theoretical studies on the carbonyl halide-water complexes, FXCO-H_2O (X = F, Cl) have found two potential minima at the MP2 and B3LYP level. Complex I forms C=O···H hydrogen bond with the planar conformation where stretching vibrations involved in hydrogen bonding are shifted to lower frequencies with enhancement of infrared intensities, corresponding to the bond elongation. The more stable complex II has the

non-hydrogen bonded angular conformation. Structural changes from monomers are small compared with complex I. The B3LYP calculation underestimates the complexation energies and predicts longer intermolecular distances compared with the MP2 calculation. NBO analysis revealed intermolecular charge transfer occur followed by intramolecular charge rearrangement. Significant charge transfer from the carbonyl oxygen lone pairs to water $\sigma^*_{O\text{-}H}$ for complex I and from one of the water oxygen lone pairs to the $\pi^*_{C=O}$ for complex II takes place. The overall charge transfer was from F_2CO to H_2O for complex I and from H_2O to F_2CO for complex II.

This work was partly supported by the Grant-in-Aid for Encouragement of Young Scientists (No. 14750574) from the Ministry of Education, Culture, Sports, Science, and Technology of Japan.

References

[1] A. McCulloch, J. Fluor. Chem. 100 (1999) 163.

[2] A. McCulloch, J. Fluor. Chem. 123 (2003) 21.

[3] S.J. Tavener, J.H. Clark, J. Fluor. Chem. 123 (2003) 31.

[4] F. Wu, R.W. Carr, J. Phys. Chem. 96 (1992) 1743.

[5] X. Cheng, Y. Zhao, Z. Zhou, J. Mol. Struct. (Theochem) 673 (2004) 43.

[6] R.V. Olkhov, I.W.M. Smith, Phys. Chem. Chem. Phys. 5 (2003) 3436.

[7] F. Cavalli, M. Glasius, J. Hjorth, B. Rindone, N.R. Jensen, Atomos. Environ. 32 (1998) 3767.

[8] Y. Inoue, M. Kawasaki, T.J. Wallington, M.D. Hurley, Chem. Phys. Lett. 343 (2001) 296.

[9] R. Zander, C.P. Rinsland, E. Mahieu, M.R. Gunson, C.B. Farmer, M.C. Abrams, M.K.W. Ko, J. Geophys. Res. 99 (1994) 16737.

[10] R.H. Judge, D.C. Moule, J. Chem. Phys. 78 (1983) 4806.

[11] I. Zanon, G. Giacometti, D. Picciol, Spectochim. Acta 19 (1963) 301.

[12] S.R. LaPaglia, A.B.F. Duncan, J. Chem. Phys. 34 (1961) 125.

[13] A. Nölle, C. Krumscheid, H. Heydtmann, Chem. Phys. Lett. 299 (1999) 561.

[14] M. Hermann, A. Nölle, H. Heydtmann, Chem. Phys. Lett. 226 (1994) 559.

[15] M. Jäger, H. Heydtmann, C. Zetzsch, Chem. Phys. Lett. 263 (1996) 817.

[16] C. Maul, K.-H. Gericke, J. Phys. Chem. A 104 (2000) 2531.

[17] C. Maul, T. Hass, K.–H. Gericke, J. Phys. Chem. A 101 (1997) 6619.

[18] M.R. Zachariah, W. Tsang, P.R. Westmoreland, D.R.F. Burgess, Jr., J. Phys. Chem. 99 (1995) 12512.

[19] N. Tanaka, T. Tamezane, H. Nishikiori, T. Fujii, J. Mol. Struct. (Theochem) 21 (2003) 631.

[20] G.C. Pimentel, A.L. McClellan, The Hydrogen Bond, Freeman, San Francisco, 1960.

[21] G.R. Desiraju, T. Steiner, The Weak Hydrogen Bond, Oxford University Press, Oxford, 1999.

[22] G.A. Jeffrey, An Introduction to Hydrogen Bonding, Oxford University Press, New York, 1997.

[23] S. Scheiner, Hydrogen Bonding, Oxford University Press, New York, 1997.

[24] I.M. Svishchev, R.J. Boyd, J. Phys. Chem. A 102 (1998) 7294.

[25] J.A. Shea, E.J. Campbell, J. Chem. Phys. 79 (1983) 4724.

[26] A.A. Stolov, W.A. Herrebout, B.J. Van der Veken, J. Phys. Chem. A 103 (1999) 5291.

[27] Y. Bouteiller, O. Abdelaoui, A. Schriver, L. Schriver-Mazzuoli, J. Chem. Phys. 102 (1995) 1731.

[28] L. Andrews, M. Hawkins, R. Withnall, Inorg. Chem. 24 (1985) 4234.

[29] A.A. Granovsky, www http://classic.chem.msu.su/gran/gamess/index.html.

[30] M.W. Schmidt, K.K. Baldridge, J.A. Boatz, S.T. Elbert, M.S. Gordon, J.J. Jensen, S. Koseki, N. Matsunaga, K.A. Nguyen, S. Su, T.L. Windus, M. Dupuis, J.A. Montgomery, J. Comput. Chem. 14 (1993) 1347.

[31] M.J. Frisch, G.W. Trucks, H.B. Schlegel, G.E. Scuseria, M.A. Robb, J.R. Cheeseman, J.A. Montgomery, Jr., T. Vreven, K.N. Kudin, J.C. Burant, J.M. Millam, S.S. Iyengar, J. Tomasi, V. Barone, B. Mennucci, M. Cossi, G. Scalmani, N. Rega, G.A. Petersson, H. Nakatsuji, M. Hada, M. Ehara, K. Toyota, R. Fukuda, J. Hasegawa, M. Ishida, T. Nakajima, Y. Honda, O. Kitao, H. Nakai, M. Klene, X. Li, J.E. Knox, H.P. Hratchian, J.B. Cross, C. Adamo, J. Jaramillo, R. Gomperts, R.E. Stratmann, O. Yazyev, A.J. Austin, R. Cammi, C. Pomelli, J.W. Ochterski, P.Y. Ayala, K. Morokuma, G.A. Voth, P. Salvador, J.J. Dannenberg, V.G. Zakrzewski, S. Dapprich, A.D. Daniels, M.C. Strain, O. Farkas, D.K. Malick, A.D. Rabuck, K. Raghavachari, J.B. Foresman, J.V. Ortiz, Q. Cui, A.G. Baboul, S. Clifford, J. Cioslowski, B.B. Stefanov, G. Liu, A. Liashenko, P. Piskorz, I. Komaromi, R.L. Martin, D.J. Fox, T. Keith, M.A. Al-Laham, C.Y. Peng, A. Nanayakkara, M. Challacombe, P.M.W. Gill, B. Johnson, W. Chen, M.W. Wong, C. Gonzalez, J.A. Pople, Gaussian 03, Revision B.03, Gaussian, Inc., Pittsburgh PA, 2003.

[32] R.A. Kendall, T.H. Dunning, Jr., R.J. Harrison, J. Chem. Phys. 96 (1992) 6796.

[33] D.E. Woon, T.H. Dunning, Jr., J. Chem. Phys. 98 (1993) 1358.

[34] Molecular Science Computing Facility, Environmental and Molecular Sciences Laboratory which is part of the Pacific Northwest Laboratory, P.O. Box 999, Richland,

Washington 99352, USA, and funded by the U.S. Department of Energy. The Pacific Northwest Laboratory is a multi-program laboratory operated by Battelle Memorial Institue for the U.S. Department of Energy under contract DE-AC06-76RLO 1830. Contact David Feller or Karen Schuchardt for further information.

[35] A.E. Reed, L.A. Curtiss, F. Weinhold, Chem. Rev. 88 (1988) 899.

[36] S.F. Boys, F. Bernardi, Mol. Phys. 19 (1970) 553.

[37] M. Nakata, K. Kohata, T. Fukuyama, K. Kuchitsu, C. J. Wilkins, J. Mol. Struct. 68 (1980) 271.

[38] N. Heineking, W. Jager, M.C.L. Gerry, J. Mol. Spectrosc. 158 (1993) 69.

[39] S. Kristyán, P. Pulay, Chem. Phys. Lett. 229 (1994) 175.

[40] K.A. Peterson, D.E. Woon, T.H. Dunning, Jr., J. Chem. Phys. 100 (1994) 7410.

[41] T. Shimanouchi, Tables of Molecular Vibrational Frequencies Consolidated Volume I, National Bureau of Standards, 1972, 1-160.

[42] A.M. Nielsen, T.G. Burke, P.J.H. Woltz, E.A. Jones, J. Chem. Phys. 20 (1952) 596.

[43] Y. Dimitrova, J. Mol. Struct. (Theochem) 391 (1997) 251.

Figure captions

Fig. 1. Optimized geometries of the FXCO-H_2O (a) complex I and (b) complex II calculated at the MP2/aug-cc-pVTZ level of theory. Intermolecular distances are denoted in Å. Upper, F_2CO-H_2O. Lower, FClCO-H_2O.

Fig. 2. Potential energies as a function of dihedral angle $\varphi_{C1O5H6H7}$ for the complex II of F_2CO (○), FClCO (□) and Cl_2CO (Δ) calculated at the CCSD(T)/6-311++(2d,2p) level.

Fig. 3. Intermolecular potential energies for the complex II of F_2CO (○), FClCO (□) and Cl_2CO (Δ) calculated at the MP2/6-311++(2d,2p) level.

Fig. 4. Electrostatic potential surfaces at 0.015 a.u. for (a) F_2CO, (b) FClCO and (c) Cl_2CO. Upper and lower represent the top and side views of the surface for the molecular plane, respectively.

Table 1

Geometry parameters of F_2CO and FClCO

Parameter[a]	MP2		B3LYP	Exp[b]
	6-311++G(2d,2p)	aug-cc-pVTZ	aug-cc-pVTZ	
F_2CO				
Bond length				
r_{CF}	1.321	1.316	1.319	1.3157
r_{CO}	1.177	1.178	1.171	1.1717
Angle				
θ_{FCO}	126.2	126.2	126.2	126.15
θ_{FCF}	107.6	107.5	107.7	107.71
Dihedral angle				
φ_{COFF}	0.0	0.0	0.0	0.0
FClCO				
Bond length				
r_{CF}	1.334	1.330	1.331	1.324
r_{CCl}	1.737	1.724	1.743	1.733
r_{CO}	1.180	1.181	1.172	1.172
Angle				
θ_{FCO}	124.1	124.2	124.2	124.70
θ_{ClCO}	126.5	126.6	126.5	126.1
θ_{FCCl}	109.3	109.3	109.3	109.22
Dihedral angle				
φ_{COFCl}	0.0	0.0	0.0	0.0

[a] Bond lengths and angles are in Å and degrees, respectively.

[b] For F_2CO from Ref. [37] and FClCO from Ref. [38].

Table 2

Geometry parameters of the F_2CO-H_2O complexes computed at the MP2 and B3LYP levels of theory[a]

Parameters[b]	Complex I						Complex II					
	MP2/6-311++G(2d2p)		MP2/aug-cc-pVTZ		B3LYP/aug-cc-pVTZ		MP2/6-311++G(2d2p)		MP2/aug-cc-pVTZ		B3LYP/aug-cc-pVTZ	
Bond length												
r_{C1F3}	1.314	(–0.0068)	1.310	(–0.0065)	1.313	(–0.0063)	1.320	(–0.0002)	1.315	(–0.0007)	1.319	(–0.0003)
r_{C1F4}	1.316	(–0.0046)	1.312	(–0.0046)	1.315	(–0.0044)	1.317	(–0.0034)	1.313	(–0.0033)	1.316	(–0.0030)
r_{C1O2}	1.181	(+0.0037)	1.181	(+0.0036)	1.175	(+0.0037)	1.178	(+0.0013)	1.179	(+0.0014)	1.173	(+0.0016)
r_{O5H6}	0.960	(+0.0023)	0.964	(+0.0025)	0.964	(+0.0024)	0.959	(+0.0010)	0.962	(+0.0009)	0.962	(+0.0005)
r_{O5H7}	0.958	(–0.0005)	0.961	(–0.0005)	0.961	(–0.0007)	0.958	(+0.0004)	0.961	(+0.0001)	0.962	(–0.0001)
Angle												
θ_{F3C1O2}	126.1	(–0.12)	126.1	(–0.09)	126.1	(–0.06)	125.9	(–0.26)	126.0	(–0.25)	125.9	(–0.24)
θ_{F4C1O2}	125.7	(–0.54)	125.7	(–0.57)	125.6	(–0.53)	126.2	(–0.01)	126.2	(–0.05)	126.1	(–0.03)
θ_{F3C1F4}	108.3	(+0.65)	108.2	(+0.65)	108.3	(+0.72)	107.8	(+0.21)	107.8	(+0.23)	107.9	(+0.22)
θ_{H6O5H7}	104.6	(+0.29)	104.4	(+0.28)	105.3	(+0.22)	104.8	(+0.51)	104.7	(+0.56)	105.5	(+0.43)
θ_{H6O5O2}	9.8		8.9		8.2							
θ_{H6O5C1}							103.8		101.3		102.3	
Dihedral angle												
$\varphi_{C1O2F3F4}$	0.0	(0.00)	0.0	(0.00)	0.0	(0.00)	–1.8	(–1.78)	–1.9	(–1.87)	–1.8	(–1.79)
$\varphi_{C1O2O5H6}$							–172.2		–172.8		–175.5	
$\varphi_{C1O5H6H7}$							139.9		144.3		139.9	
distance												
r_{C1O5}	3.759		3.764		3.878		2.666		2.644		2.773	

r_{O2O5}	3.052	3.033	3.089	2.991	2.950	3.080
r_{O2H6}	2.112	2.086	2.139	2.993	2.905	3.064

[a] Changes in values from the corresponding monomer are given in parentheses.

[b] Bond lengths and angles are in Å and degrees, respectively.

Table 3

Geometry parameters of the FClCO-H_2O complexes computed at the MP2 and B3LYP levels of theory[a]

Parameters[b]	Complex I						Complex II					
	MP2/6-311++G(2d2p)		MP2/aug-cc-pVTZ		B3LYP/aug-cc-pVTZ		MP2/6-311++G(2d2p)		MP2/aug-cc-pVTZ		B3LYP/aug-cc-pVTZ	
Bond length												
r_{C1F3}	1.328	(–0.0064)	1.324	(–0.0061)	1.325	(–0.0056)	1.332	(–0.0017)	1.327	(–0.0027)	1.329	(–0.0020)
r_{C1Cl4}	1.730	(–0.0070)	1.717	(–0.0066)	1.736	(–0.0067)	1.735	(–0.0025)	1.721	(–0.0027)	1.741	(–0.0022)
r_{C1O2}	1.184	(+0.0040)	1.185	(+0.0038)	1.176	(+0.0039)	1.181	(+0.0011)	1.182	(+0.0015)	1.174	(+0.0014)
r_{O5H6}	0.961	(+0.0024)	0.964	(+0.0026)	0.964	(+0.0024)	0.959	(+0.0011)	0.963	(+0.0012)	0.962	(+0.0006)
r_{O5H7}	0.958	(–0.0005)	0.961	(–0.0005)	0.961	(–0.0006)	0.959	(+0.0004)	0.962	(+0.0003)	0.962	(–0.0001)
Angle												
θ_{F3C1O2}	123.9	(–0.26)	123.9	(–0.24)	124.0	(–0.18)	124.0	(–0.11)	124.1	(–0.10)	124.1	(–0.08)
$\theta_{Cl4C1O2}$	126.1	(–0.40)	126.2	(–0.43)	126.1	(–0.39)	126.4	(–0.10)	126.4	(–0.15)	126.4	(–0.12)
$\theta_{F3C1Cl4}$	110.0	(+0.66)	109.9	(+0.64)	109.9	(+0.57)	109.5	(+0.18)	109.5	(+0.21)	109.5	(+0.17)
θ_{H6O5H7}	104.4	(+0.18)	104.3	(+0.23)	105.2	(+0.10)	104.7	(+0.40)	104.6	(+0.50)	105.4	(+0.32)
θ_{H6O5O2}	5.4		5.8		4.3							
θ_{H6O5C1}							97.8		92.9		92.7	
Dihedral angle												
$\varphi_{C1O2F3Cl4}$	0.0	(0.00)	0.0	(0.00)	0.0	(0.00)	–1.4	(–1.43)	–1.4	(–1.37)	–1.3	(–1.27)
$\varphi_{C1O2O5H6}$							–169.1		–169.4		–170.9	
$\varphi_{C1O5H6H7}$							141.0		152.2		140.0	
Distance												
r_{C1O5}	3.861		3.875		3.978		2.773		2.758		2.942	

r_{O2O5}	3.060	3.044	3.104	3.000	2.937	3.110
r_{O2H6}	2.106	2.087	2.144	2.904	2.752	2.938

[a] Changes in values from the corresponding monomer are given in parentheses.

[b] Bond lengths and angles are in Å and degrees, respectively.

Table 4

BSSE corrected interaction energies (kcal mol^{-1}) of the FXCO-H_2O complexes

	F_2CO		FClCO	
	complex I	complex II	complex I	complex II
HF				
6-311++G(2d,2p)	–1.58	–2.77	–1.64	–1.87
aug-cc-pVTZ	–1.65	–2.78	–1.71	–1.81
aug-cc-pVQZ	–1.68	–2.80	–1.76	–1.82
aug-cc-pV5Z	–1.69	–2.81	–1.76	–1.83
MP2				
6-311++G(2d,2p)	–2.18	–3.32	–2.13	–2.73
aug-cc-pVTZ	–2.50	–3.89	–2.45	–3.28
aug-cc-pVQZ[a]	–2.61	–4.06	–2.56	–3.42
aug-cc-pV5Z[a]	–2.64	–4.13	–2.58	–3.48
CBS[a,b]	–2.66	–4.17	–2.59	–3.52
MP4SDTQ				
6-311++G(2d,2p)[c]	–2.21	–3.30	–2.18	–2.67
CCSD(T)				
6-311++G(2d,2p)[c]	–2.21	–3.33	–2.21	–2.65
B3LYP				
aug-cc-pVTZ	–2.28	–2.92	–2.14	–1.98

[a] Geometries obtained at the MP2/aug-cc-pVTZ level.

[b] $E(X) = E_{CBS} + Ae^{-(X-1)} + Be^{-(X-1)^2}$

[c] Geometries obtained at the MP2/6-311++G(2d,2p) level.

Table 5

Unscaled harmonic vibrational frequencies (cm^{-1}) and intensities ($km\ mol^{-1}$) of monomers calculated at the MP2/aug-cc-pVTZ and B3LYP/aug-cc-pVTZ level of theory[a]

mode	MP2		B3LYP		Exp[a]	
	ν	I	ν	I	ν	I
H_2O						
OH_2 a-str	3948.2	75.0	3898.9	63.0	3755.79	
OH_2 s-str	3818.0	6.4	3796.2	4.6	3656.65	
OH_2 bend	1623.2	72.0	1627.0	75.8	1594.59	
F_2CO						
C=O str	1949.2	431.7	1958.2	474.6	1928	VS
CF_2 a-str	1249.6	416.9	1218.1	423.4	1249	VS
CF_2 s-str	972.7	65.3	963.5	60.5	965	VS
Oop	785.1	32.2	776.2	35.0	774	M
CO deform	615.6	6.3	615.9	5.9	626	M
CF_2 bend	584.5	6.4	576.0	5.0	584	M
FClCO						
CO str	1881.7	350.4	1908.5	410.9	1868	VS
CF str	1097.1	415.2	1075.6	417.1	1095	S
CCl str	767.3	85.0	754.1	90.6	776	M
Oop	675.4	13.0	670.6	14.8	667	M
CO deform	508.9	0.3	489.4	1.1	501	W
CFCl bend	413.2	0.5	405.3	0.4	415	VW

[a] For H_2O from Ref. [41], and for F_2CO and FClCO from Ref. [42].

Table 6

Unscaled harmonic vibrational frequencies (cm^{-1}) and intensities ($km\ mol^{-1}$) of the F_2CO-H_2O complexes calculated at the MP2/aug-cc-pVTZ level of theory[a]

mode	Complex I				Complex II			
	ν		I		ν		I	
OH a-str	3931.0	(–17.2)	178.2	(+103.3)	3932.6	(–15.6)	84.5	(+9.5)
OH s-str	3805.7	(–12.3)	83.1	(+76.6)	3797.1	(–20.9)	15.1	(+8.7)
HOH bend	1633.0	(+9.9)	62.0	(–10.0)	1624.5	(+1.3)	86.9	(+14.9)
CO str	1941.1	(–8.1)	493.5	(+61.8)	1947.3	(–2.0)	417.7	(–14.0)
CF_2 a-str	1279.8	(+30.2)	400.2	(–16.7)	1260.6	(+11.0)	393.9	(–23.0)
CF_2 s-str	980.1	(+7.5)	57.5	(–7.8)	976.3	(+3.7)	57.5	(–7.7)
Op deform	790.3	(+5.2)	34.2	(+2.0)	770.3	(–14.8)	61.5	(+29.3)
CO deform	623.2	(+7.6)	8.1	(+1.8)	618.8	(+3.2)	6.4	(+0.2)
CF_2 deform	587.6	(+3.1)	4.6	(–1.8)	585..2	(+0.7)	5.3	(–1.1)

[a] Changes in values from the corresponding monomer are given in parentheses.

Table 7

Unscaled harmonic vibrational frequencies (cm^{-1}) and intensities ($km\ mol^{-1}$) of the FClCO-H_2O complexes calculated at the MP2/aug-cc-pVTZ level of theory[a]

mode	Complex I				Complex II			
	ν		I		ν		I	
OH a-str	3939.4	(–8.9)	193.4	(+118.4)	3911.7	(–36.6)	81.0	(+6.0)
OH s-str	3811.8	(–6.2)	117.3	(+110.8)	3784.2	(–33.8)	10.2	(+3.8)
HOH bend	1634.9	(+11.7)	54.6	(–17.4)	1624.8	(+1.6)	99.3	(+27.4)
CO str	1866.6	(–15.1)	422.5	(+72.1)	1881.0	(–0.7)	338.5	(–11.9)
CF str	1128.3	(+31.2)	396.5	(–18.7)	1110.2	(+13.2)	401.8	(–13.4)
CCl str	772.9	(+5.5)	81.7	(–3.4)	773.9	(+6.6)	78.1	(–6.9)
Op deform	679.4	(+3.9)	15.1	(+2.1)	667.0	(–8.5)	24.8	(+11.8)
CO deform	513.6	(+4.7)	0.5	(+0.1)	507.1	(–1.8)	0.3	(0.0)
CFCl deform	418.7	(+5.5)	0.3	(–0.2)	415.3	(+2.1)	0.6	(+0.1)

[a] Changes in values from the corresponding monomer are given in parentheses.

Table 8

Natural atomic charges of monomers and changes in natural atomic charges of the FXCO-H_2O complexes

atom	Δq / me		q / e
	complex I	complex II	monomer
F_2CO-H_2O			
C1	16.67	30.30	1.31821
O2	–31.55	–34.78	–0.61274
F3	11.37	–2.10	–0.35274
F4	7.13	2.69	–0.35273
O5	–19.42	–10.49	–0.93008
H6	18.94	8.73	0.46504
H7	–3.13	5.65	0.46504
FClCO-H_2O			
C1	12.09	25.11	0.97059
O2	–33.82	–29.81	–0.58858
F3	9.96	–1.47	–0.36698
Cl4	15.6	2.3	–0.01502
O5	–18.85	–14.5	–0.93008
H6	19.06	11.03	0.46504
H7	–4.05	7.33	0.46504

Table 9

Charge transfer interactions in complex I

Parameter[a]	F_2CO-H_2O	$FClCO$-H_2O
Intermolecular		
$E^{(2)}\ n_{1\ O2} \rightarrow \sigma^*_{\ O5\text{-}H6}$	1.0	1.0
$E^{(2)}\ n_{2\ O2} \rightarrow \sigma^*_{\ O5\text{-}H6}$	2.0	1.7
Intramolecular		
$\Delta E^{(2)}\ n_{2\ O2} \rightarrow \sigma^*_{\ C1\text{-}F3}$	–2.2	–2.6
$\Delta E^{(2)}\ n_{2\ O2} \rightarrow \sigma^*_{\ C1\text{-}X4}$	–2.6	–2.6
$\Delta E^{(2)}\ n_{3\ F3} \rightarrow \pi^*_{\ C1\text{-}O2}$	+1.0	+2.1
$\Delta E^{(2)}\ n_{3\ X4} \rightarrow \pi^*_{\ C1\text{-}O2}$	+0.3	+1.8
$\Delta n_{2\ O2}$	+8.2	+9.2
$\Delta n_{3\ F3}$	–4.2	–4.0
$\Delta n_{3\ X4}$	–3.0	–4.8
$\Delta\sigma^*_{\ C1\text{-}O2}$	+3.2	+1.2
$\Delta\pi^*_{\ C1\text{-}O2}$	+5.3	+8.5
$\Delta\sigma^*_{\ C1\text{-}F3}$	–5.0	–5.0
$\Delta\sigma^*_{\ C1\text{-}X4}$	–4.3	–5.5
$\Delta\sigma^*_{\ O5\text{-}H6}$	+3.5	+3.5

[a] The second-order perturbation energies are given in kcal mol^{-1}. The changes in the orbital population are given in me.

Table 10

Charge transfer interactions in complex II

Parameter[a]	F_2CO-H_2O	$FClCO$-H_2O
Intermolecular		
$E^{(2)}\ n_{2\ O5} \rightarrow \pi^*_{C1\text{-}O2}$	2.55	1.97
$E^{(2)}\ \pi_{C1\text{-}O2} \rightarrow \sigma^*_{O5\text{-}H7}$	0.24	0.25
Intramolecular		
$\Delta E^{(2)}\ n_{2\ O2} \rightarrow \sigma^*_{C1\text{-}F3}$	+1.68	–0.64
$\Delta E^{(2)}\ n_{2\ O2} \rightarrow \sigma^*_{C1\text{-}X4}$	+1.13	–0.25
$\Delta E^{(2)}\ n_{3\ F3} \rightarrow \pi^*_{C1\text{-}O2}$	+1.44	+0.88
$\Delta E^{(2)}\ n_{3\ X4} \rightarrow \pi^*_{C1\text{-}O2}$	+2.22	+0.53
$\Delta n_{2\ O2}$	+2.5	+2.3
$\Delta\sigma^*_{C1\text{-}O2}$	+1.2	+1.0
$\Delta\pi^*_{C1\text{-}O2}$	+5.7	+5.1
$\Delta\sigma^*_{C1\text{-}F3}$	+1.2	–0.52
$\Delta\sigma^*_{C1\text{-}X4}$	–0.3	–0.48
$\Delta n_{2\ O5}$	–5.1	–3.0

[a] The second-order perturbation energies are given in kcal mol^{-1}. The changes in the orbital population are given in me.

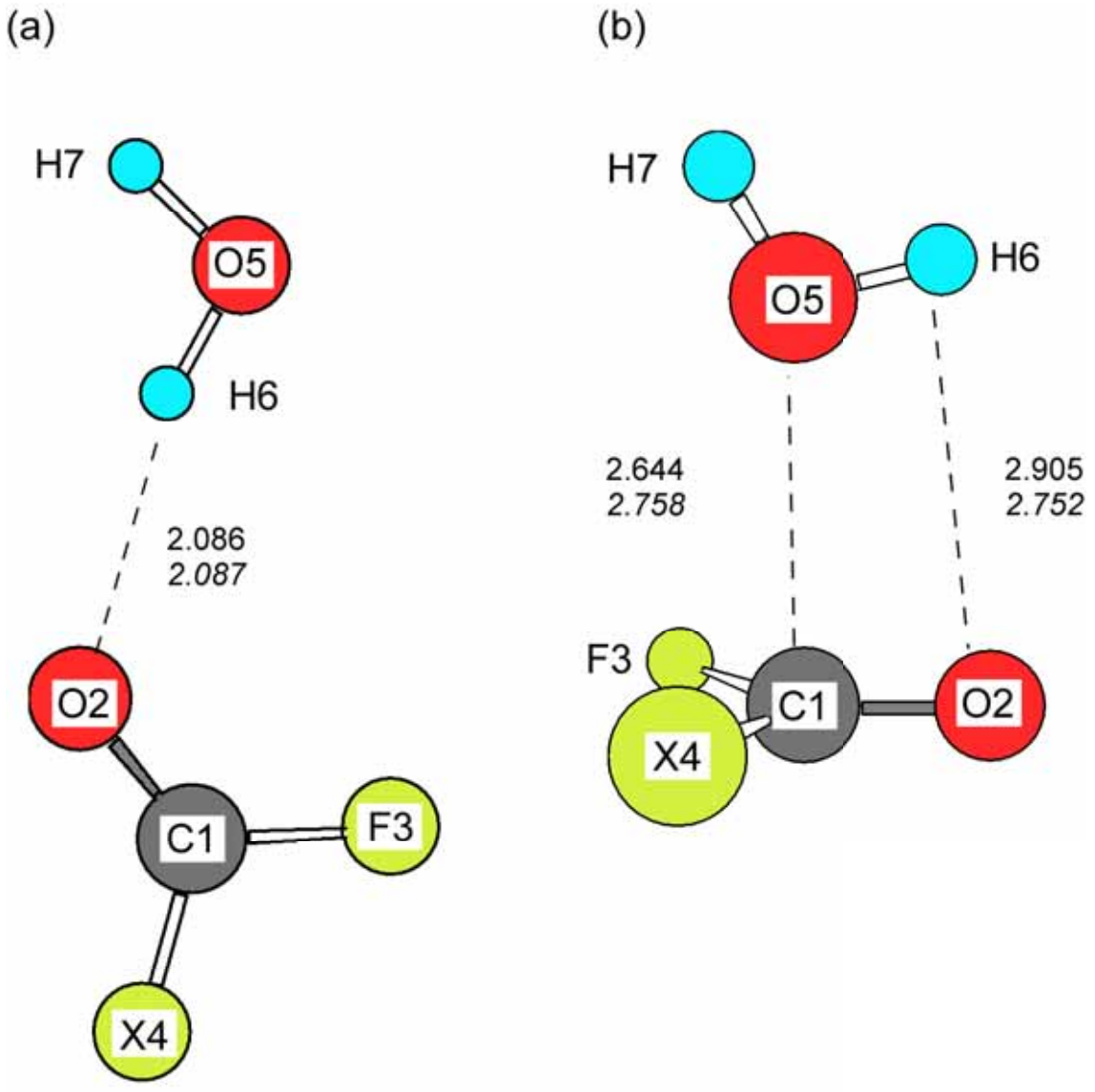

Fig. 1. Tanaka et al. “Theoretical studies on carbonyl halide-water complexes”

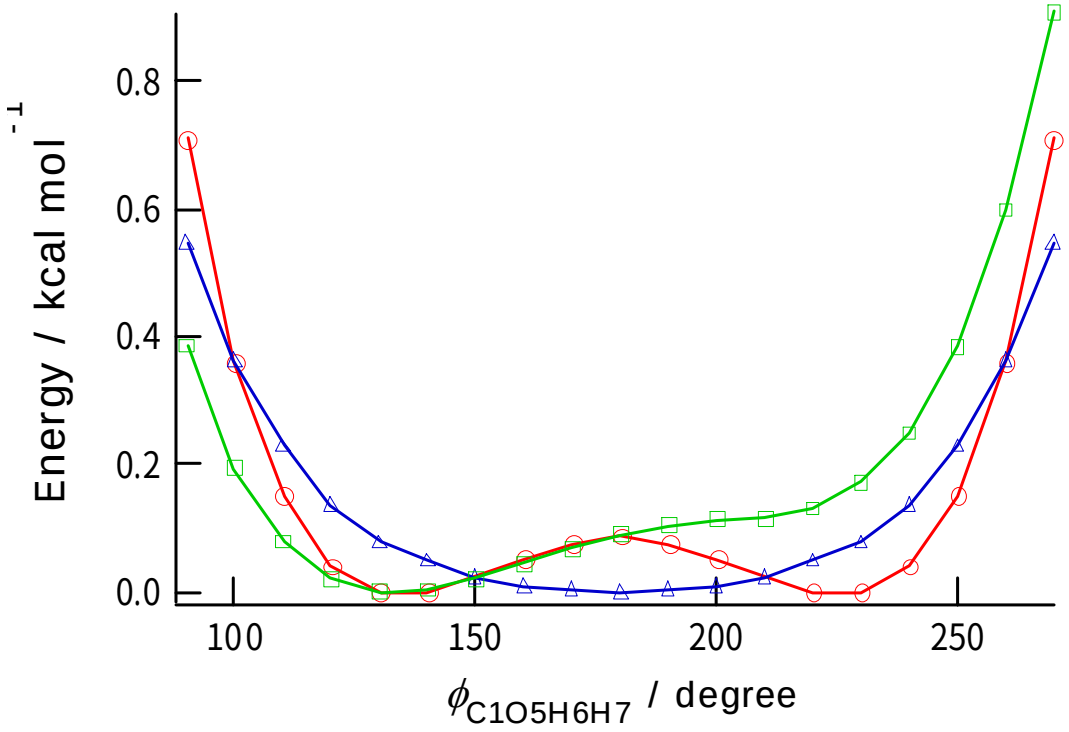

Fig. 2. Tanaka et al. “Theoretical studies on carbonyl halide-water complexes”

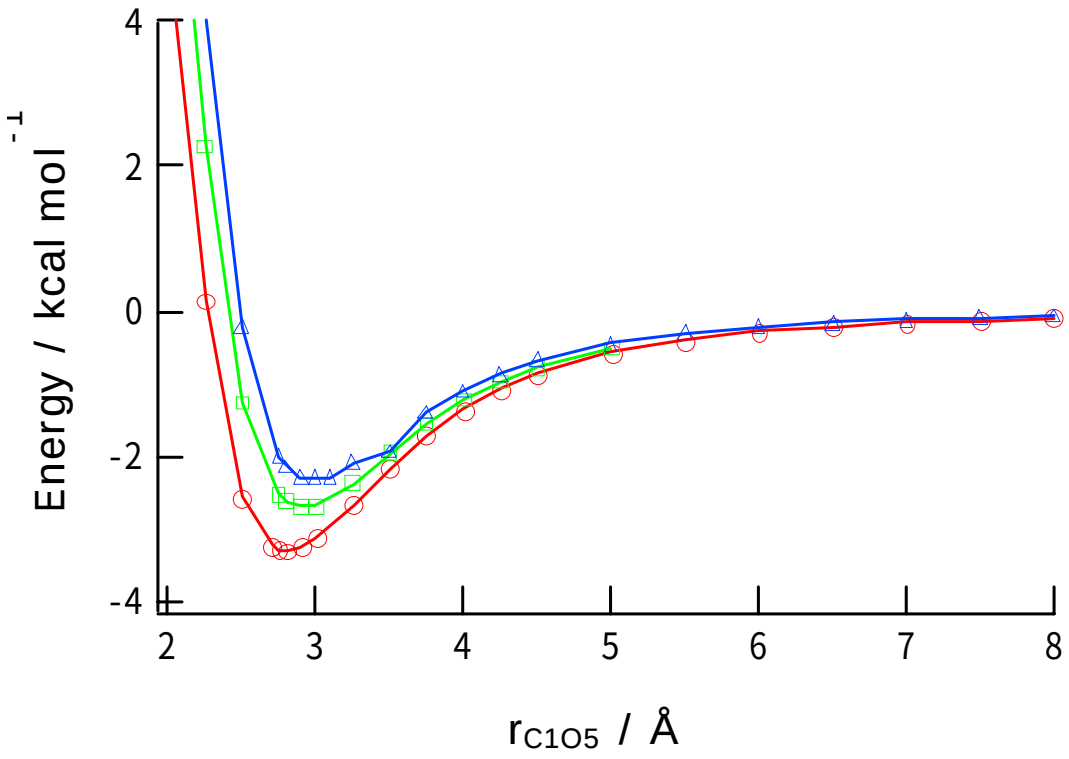

Fig. 3. Tanaka et al. “Theoretical studies on carbonyl halide-water complexes”

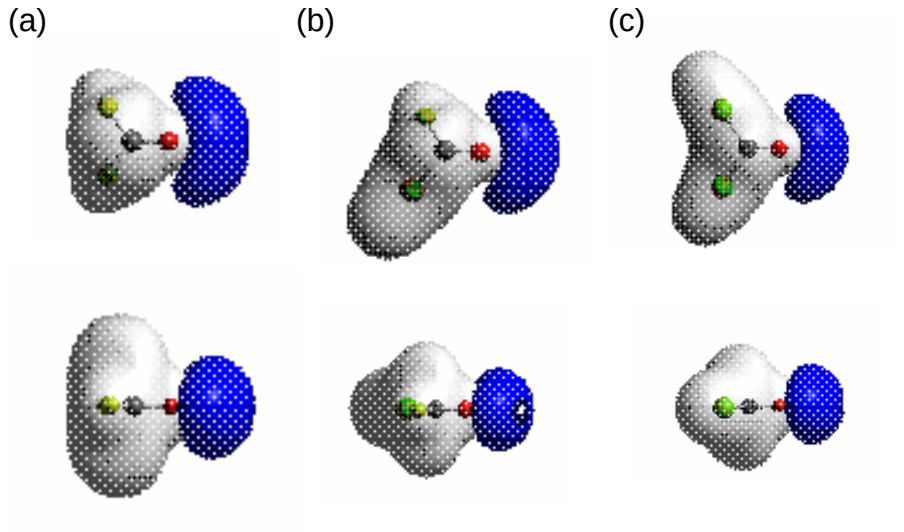

Fig. 4. Tanaka et al. “Theoretical studies on carbonyl halide-water complexes”